

COVER PAGE

Document downloaded by @DAEL

Sat Nov 28 22:34:20 2026
For personal use

When automatic English translation is provided, only the original document is authentic.
The EAA cannot be held responsible of any translation error

Bibliographical reference

Edge Boundary Conditions Impact on the Radiation of Multiactuator Panels for Multichannel Audio Reproduction, Basilio Pueo, José J. López and José Escolano, Acta Acustica **vol. 94** (Number 5), 2008, pp. 754-764

DOI
https://doi.org/10.3813/AAA.918093

ACTA ACUSTICA UNITED WITH ACUSTICA
Vol. 94 (2008) 754 – 764
DOI 10.3813/AAA.918093

Edge Boundary Conditions Impact on the Radiation of Multiactuator Panels for Multichannel Audio Reproduction

Basilio Pueo[1], José J. López[2], José Escolano[2,3]
[1] Signals, Systems and Telecommunications Group, Polytechnic School, University of Alicante, Spain.
basilio@ua.es
[2] Institute of Telecommunications and Multimedia Applications, Technical University of Valencia, Spain.
jjlopez@dcom.upv.es
[3] Telecommunication Engineering Department, Polytechnic School, University of Jaén, Spain.
escolano@ujaen.es

Summary
An empirical study of the impact that the edge boundary conditions have on the radiated wave field for Multiactuator Panels (MAP) is presented. The aim is not the underlying physics on plate theory, but to experiment with practical boundary conditions to form a viable technology for a MAP frame in multichannel audio reproduction systems. Besides classical clamped and free boundary conditions, three types of elastic boundaries have been addressed as viable edge boundary conditions. Two elastic materials have been chosen as representative of flexible and hard types within the commercial range to develop the elastic boundaries. In addition to the on-axis and directivity responses, microphone array measurements have been interpreted in the wavenumber domain, where the source radiation is analyzed in space and time. Results show significant differences on varying the panel boundary conditions and elastic materials under test.
PACS no. 43.38.Hz, 43.38.Md, 43.60.Gk

1. Introduction

In recent years, Distributed Mode Loudspeakers (DML) are becoming a planar radiator alternative to the widespread piston-like loudspeakers. A DML consists of a thin panel that is set into vibration by means of a special electroacoustic transducer called an exciter [1]. DMLs can easily be integrated into a living room because of its low visual profile [2, 3]. Furthermore, the vibration of the surface is almost negligible so that it can be used as projection screens [4]. Due to these properties, DMLs have been proposed as loudspeaker arrays for Multichannel Audio Systems, such as Wave Field Synthesis (WFS) [5, 6] or Ambisonics [7], in which a set of exciters is attached to a single vibrating surface and drives an independent signal to create a given acoustic field. In this context, Multiexcited DMLs are known as Multiactuator Panels or MAP [8, 9].

The accommodation of several transducers in a single panel introduces some changes with respect to the single exciter DML. First, the panel material needs to be stiffer to achieve independency between exciters vibration [9]. Furthermore, in WFS, the exciter points must be equidistantly located on a horizontal line in the panel. Hence, the combination of optimum panel aspect ratios and drive points of a single exciter DML that produces an even distribution of modes and a higher modal density cannot now be observed. Besides, to create a large listening area, panels need to be attached on the reproduction line side, which forced to locate the first and last exciters very close to the panel edges [8]. In this frame, the behaviour of the panel at the edges is of great importance and may influence the radiation characteristics.

In this paper, the impact that the edge boundary conditions have on the radiated wave field is addressed through an empirical study. Some preliminary results for clamped and elastic boundaries were presented in [10]. The purpose of this work is not the underlying physics on plate theory, but to experiment with practical boundary conditions to form a viable technology for a MAP frame. Since the panel is usually placed in a baffle to avoid back to front cancellation, its edges must be supported in the frame in some boundary condition. This works focuses on the elastic boundaries for their flexible features. Two elastic materials have been used as representative of the range of available materials to support the panel. In addition, the classical clamped and free boundary conditions have also been tested in the laboratory for comparison purposes.

The outline of the paper is presented as follows. An overview of the distributed mode operation for single-

Received 8 April 2008, revised 18 July 2008,
accepted 20 August 2008.

© S. Hirzel Verlag · EAA

and multiple-excited loudspeaker panels is given in section 2. Section 3 discusses the different ways of attaching the panel to the frame along the edges. Both pure boundary conditions, such as clamped or free, and three boundary conditions based on elastic boundaries, are presented. The experimental setup is detailed in section 4. Section 5 presents experimental results and discussion of MAPs when reproducing several stimuli. On-axis and directivity responses are presented for single exciter operation. In addition, spherical and plane waves are measured in the wavenumber domain by a space and time sampling, according to the setup described in section 4. Finally, section 5 concludes the paper.

2. Loudspeaker Arrays

The output signal of multichannel audio systems is reproduced by a number of transducers distributed in a loudspeaker array. This paper addresses the arrays based on the distributed mode operation in the context of WFS reproduction. In this section, a brief description of the basics of WFS will be first introduced. Later, the single-excited DML and its transformation to an array of exciters in a single panel, known as MAP in the technical literature, will be described.

2.1. Wave Field Synthesis

WFS is a spatial reproduction technique that, by analogy to holography and in base to the Huygens principle, reproduces an acoustic field inside a volume from the stored signals recorded in a given surface. Huygens principle states that the wave front radiated by a source behaves like a distribution of sources that are in the wave front, named secondary sources.

WFS was first proposed with application to 3D sound by Berkhout [5]. The synthetic wave front is created by loudspeaker arrays that substitute the individual secondary sources. The ideal situation would be when an area, which is completely surrounded by loudspeakers, is fed with signals that create a volumetric velocity proportional to the particle velocity normal component of the original wave front.

The main advantage of these systems is that the acoustic scene has not sweet spot. When listeners move inside the listening area, the sound pressure level changes also in a realistic way according to its relative position to the virtual source. In addition to virtual sources behind the loudspeaker array, it is also possible to synthesize sources inside the listening area, known as focused sources. However, the recreation of a true natural wave field can be fulfilled with certain restrictions. Huygens principle needs to be discretized in practice, which means that an infinite continuous secondary source distribution is replaced by a number of finite arrays of equidistant discrete loudspeakers. The lack of continuity leads to a maximum usable frequency, known as spatial aliasing frequency, whereas the finiteness of the array causes some truncation effects. For a detailed description of this drawbacks within a listening room, refer to [11, 12, 13].

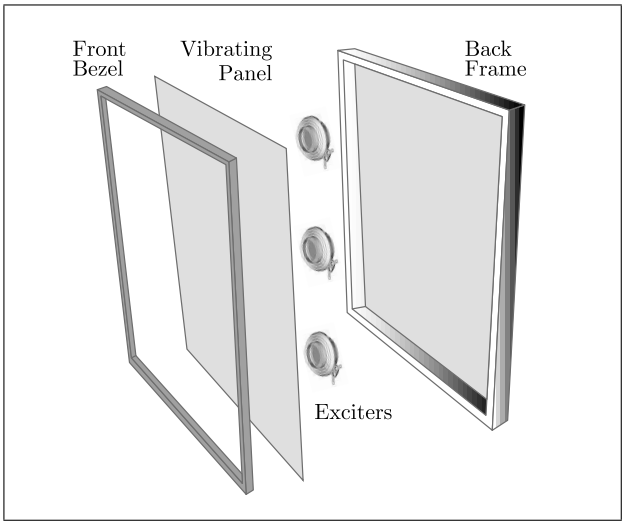

Figure 1. Graphical representation of a three-exciter multiactuator panel. Electric wiring is omitted for simplicity.

This setup is present in the loudspeaker arrays for WFS reproduction that have been designed during the past years. Basically, according to the transduction mechanism, two types of loudspeaker arrays have been developed. Firstly, arrays based on the dynamic transducer, which have extensively described in the technical literature and have been generalized for an arbitrary loudspeaker directivity in [14]. Secondly, arrays comprising several exciters onto a DML panel substituting individual loudspeakers. In the following sections, the distributed mode operation and the development to produce MAPs will be explained in detail.

2.2. Distributed Mode Loudspeaker

The DML is an electro-acoustic transducer based on the radiation of modal bending wave shapes by means of the vibration of a flat panel. This acoustic radiator arose during the investigation of lightweight composites for use in helicopters. It was found that the panels re-radiated significant output in the audio band when excited, which showed that a resonant multi-modal radiator could be used as a loudspeaker [15].

In a DML panel, the acoustic output is the sum of a large number of uncorrelated modes. For such a radiation be adequate for audio applications, the density and spacing of these modes must be suitable to produce a continuous spectrum. In this case, the fully modal, uncorrelated output is perceived by the listener as a smoothly varying response. Hence, for a right modal density, the design process involves the correct selection of the two main parts of a DML, panel and so-called exciters.

Regarding the panel, DMLs are built on light and stiff materials such as paper, aluminium, polypropylene or polycarbonate. The selection of each material is made in terms of the final application. For a proper generation of bending waves, the sandwich structure is the most spread

among designers. Whereas skins may take several forms to accomplish a given application, such as DML in a picture or as part of a wall, the core is usually a honeycomb structure or a foam.

The DML diaphragm is driven at special points by electromechanical transducer called exciters. The transducer mechanism of such an exciter is similar to that of conventional loudspeaker drivers. Dynamic type transducer is the technology mostly used, but piezoelectric transducers have also been tested, which may extend the response into the ultrasonic range, also known as Distributed Mode Actuator. A graphical representation of the comprising parts of a DML is given in Figure 1.

For a dense and even frequency distribution of modes, the excitation points are chosen in such a way so as to excite as many modes as possible. A single panel can be driven using multiple exciters with the same signal to enhance the mode generation, and increase the delivered power. Recent works have shown that is is possible to obtain an optimal exciter deployment using genetic algorithms [16], and improve the sound pressure responses with properly attached masses to the panel [17].

2.3. Multiactuator Panels

Multiactuator panels are an extension of the distribute mode technology for WFS applications. They consist of a set of exciters, evenly distributed on a line, that are attached to a single vibrating surface. Each exciter, that must act as a secondary source of the WFS algorithm, receives an independent signal to create a multichannel system. To avoid back to front cancellation, which results in a smoother frequency response, and for practical support, the panel is mounted on a housing with absorbing material [18].

MAPs present several advantages for a WFS listening area. Due to their diffuse radiation and omnidirectionality, the individual components merge correctly into the desired wavefront for a wider area. Also, being planar transducers, the pressure level decay with distance is less pronounced in comparison with typical piston-like loudspeakers. However, the modal nature of the panel creates an irregularly frequency response, with peaks and dips, that need to be equalized by appropriate filtering [19]. Also, the planar shape can introduce undesired reflections for acoustic waves which disturb the perception of the target soundfield. To solve this problem, a compensation based in the image sources method has been proposed [20]. Figure 2 shows a picture of the MAPs used for experiments.

In a single-exciter panel, the optimal positions, usually four in the center area of the panel, are chosen to excite the maximum number of vibration modes. This results in an even distribution of modes, and a high modal density, which is more noticeable in the low frequency region [21]. For WFS operation, such golden points cannot be observed since the vibration points are set by the secondary sources of the WFS algorithm. Away from the optimal points, there is no guarantee of a proper distribution of modes. Besides, for WFS operation, each exciter must only drive a small part around the exciter position, acting as discrete radiating point [8].



Figure 2. Multiactuator panels for WFS rendering experiments.

Hence, the use of these panels for WFS applications depends on the structural characteristics of the panel and exciters, which can degrade the desired wave field if not properly designed. In this regard, as stated in [9], the structural near field around the excitation point, the panel dimensions, and the exciter position can influence the generated wave field to a large extent. In addition to these structural items, the edge boundary conditions is one of the critical points that need to be evaluated and improved.

3. Panel Edge Boundary Conditions

In this section, the different ways of supporting the panel is discussed. Rectangular plates are generally classified in accordance with the type of support used [22]. The three basic boundary conditions applied to a plate edge are Free (F), Simply Supported (SS) and Clamped (C) edges, also known as built-in plates. The ideal free condition implies that the structure is floating in the air without any support of any kind. If such a condition is satisfied, no reaction forces arise along the edges: there are no bending and twisting moments, and also no shearing forces perpendicular to the support direction. At the other extreme, the clamped condition is achieved by grounding the structure with well-tightened devices that prevent the deflection of the structure at the supports. In this case, several reaction forces are created along edges: two forces, normal and perpendicular to the support direction, and a bending moment perpendicular to the plane structure. In between, there is the simply supported condition, which behaves as a clamped edge but without bending moments because edges can rotate freely with respect to the edge line.

In addition, other type of boundary conditions appear as a result of combining the above conditions [23]. For example, the mixed supported conditions have clamped, simple supported and free at different edges. There are also the point supports, which consist of a plate supported by intermediate points.

However, the boundary condition that involves some sort of elastic damping is known as Elastic Boundary (EB). Plates on elastic boundaries are supported by elastic supports which resist certain type of bending [24]. Its mechanical model is equivalent to a plate supported elastically by springs uniformly distributed along its edge. Hence, two reactions arise: deflection and edge rotation

are opposed by linear and spiral springs having a certain degree of distributed stiffness. Because of the flexible features on edges, elastic boundaries are suitable in DML loudspeakers for audio reproduction.

In the technical literature, DML and MAP models have been presented with simply supported edges: [25] (for the baffled loudspeaker) [16] (adhesive tape to fix boundaries in the laboratory), [17], or combined with free edges: [25] (for the unbaffled loudspeaker), [26].

Nevertheless, both free and simply supported edge conditions have disadvantages to form a viable technology for a MAP frame. On the one hand, the free condition can be approximated by supporting the structure on very flexible springs, which gives raise to a free radiating panel in a full-space radiation. However, when observing the typical polar response of a free DML, a reduction of pressure in the plane of the panel is noticed, due to the cancellation effect of acoustic radiation at or near the edges. For that reason, the panel is usually placed in a baffle, where radiation due to the rear part of the panel becomes contained. On the other hand, simply supported conditions must contain a certain degree of frame grounding if the panel is to be held. This problem can be confronted by pseudorandomly diffusing the boundaries between pure clamped and free, in a special type of Mixed Boundary Condition suggested by [21]. Unfortunately, such a condition does not present a reliable fixing frame since part of the panel is suspended in the air.

Because of these practical drawbacks, this work is focused on the study of elastic boundaries as edge boundary conditions that can form the basis of a closed back MAP technology. For that purpose, three configurations are analyzed, covering the practical interactions between panel edges and housing. Elastic Boundaries types 1 and 2 consist of a modification of the clamped conditions although including elastic materials in one or two sides of the panel. Elastic Boundary type 3 is formed by a simply supported edge but with an elastic material between panel and housing. In the following, elastic boundaries types 1, 2 and 3 will be referred to as EB1, EB2 and EB3, respectively. Figure 3 shows a graphical representation of clamped, free and these elastic boundaries. For comparison purposes, two different elastic materials have been used, with enough elastic differences to become representatives of hard and soft materials. Details on such elastic boundaries used in the experiments are addressed in the next section.

4. Laboratory Setup

The impact of the edge boundary conditions on the radiation of MAPs is analyzed by considering an arrangement of MAPs in the laboratory which can change their supporting properties. Then, on-axis response and directivity measurements, and a space-time wavenumber domain analysis by sampling the created wave field, is performed. A detailed description of the experimental setup is given below.

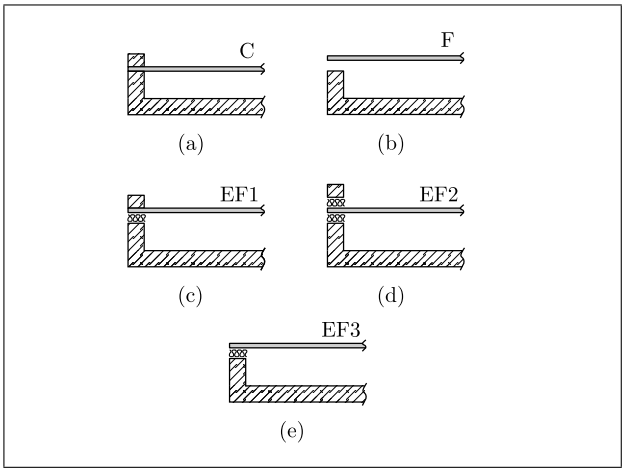

Figure 3. Section detail of the edge boundary conditions under test. (a) Clamped. (b) Free. (c) Elastic Boundary type 1. (d) Elastic Boundary type 2. (e) Elastic Boundary type 3.

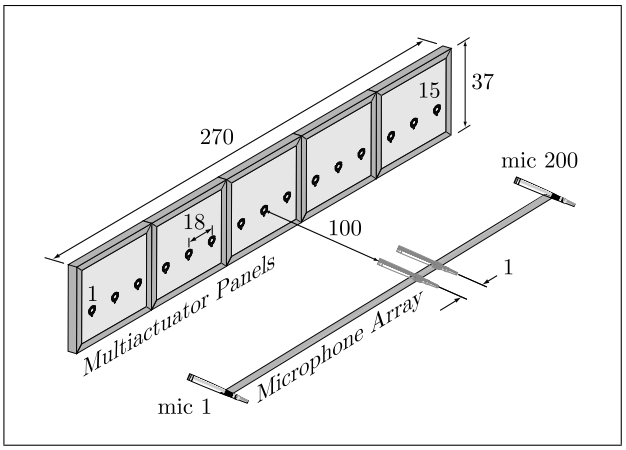

Figure 4. Experimental setup geometry for the analysis of the edge boundary conditions impact on the radiation. Dimensions in centimeters.

4.1. MAPs

The emitting stage is composed of an arrangement of five MAPs comprising three exciters per panel, as depicted in Figure 2. This setup has been designed and built in the laboratory for this particular study. With such a multiple small MAP configuration, it was intended to enhance the effect that different BC may have on the system. Alternatively, a larger MAP including the same number of exciters would only have boundaries at the extent of the panel, far beyond the position of exciters, and their impact would be more difficult to detect.

The panel is a 5 mm sandwich that connects a thermoplastic outer skin material to a polycarbonate inner honeycomb core. The panel bending stiffness is 16.4 and 16 Nm in the x and y directions respectively and has an areal density of 0.89 kg/m^2. The exciters are 25 mm diameter dynamic transducers with an eight-foot panel coupling. Details on the geometric description of the experiment setup are given in Figure 4.

4.2. Assembling Edge Boundary Conditions

As stated previously, the boundary conditions based on elastic boundaries are of great interest to produce a MAP frame technology. For comparison purposes, both clamped and free conditions have also been tested because of distinctive characteristics. Figure 3 shows a section of a single boundary having the experimental boundary conditions. Note that the MAPs in this experiment maintain the same sort of boundary condition along their four sides.

To achieve a clamped condition in the laboratory, no deflection must occur at any point along the boundary. If this requirement is not satisfied, a simply supported condition will arise instead. As a consequence, the portion of the panel to be clamped by the tight structure is more than twice the width of the panel for the experiments. On the other hand, the free condition can be approximated by suspending the panel in the air with soft rubber bands, as suggested in [27]. This suspension in the air has been applied individually to each of the five MAPs under test, avoiding contact between adjacent sides. Additionally, for a proper comparison, the back housing that is present in the rest of boundary conditions, is also considered for the free condition. To that end, the housing is placed several millimeters below the panel to absorb the back radiation while allowing free movement at edges. Special effort has been made to recreate such conditions in the laboratory so that presented measurements will reflect their impact on MAPs' radiation.

4.3. Elastic Materials

Two types of elastic materials have been employed to develop the elastic boundaries. The first one is a low-density polyethylene foam or LDPE and the second is an ethylene propylene diene monomer rubber or EPDM, both of them widely available in the market under several commercial brands. In the following, LDPE and EPDM materials will be named with the simple tags "foam" and "rubber" respectively, to avoid confusion with acronyms. For this experiment, both materials take the shape of a strip with a rectangular section (0.5 mm×1 mm).

To characterize their elastic behavior with precision, they were tested in the laboratory by a Thermomechanical Analysis (TMA) at room temperature [28]. It was intended to measure the exact conditions with which they will be used, so values obtained in the material database were not valid since they did not account for the particular shape employed. For this reason, samples of elastic material with geometrical characteristics (width, length and depth) identical to those used in MAPs were essayed under compression for observing dimensional changes in the axis where forces are applied (see Figure 5). The elastic modulus for this particular case can be described as the ratio between stress and strain. Measurements with the TMA Analyzer provided values of $21.8 \cdot 10^6$ N/m^2 for foam and $191.4 \cdot 10^6$ N/m^2 for rubber, which means that foam is the most flexible material and rubber the most rigid.



Figure 5. Thermomechanical Analyzer with a sample of elastic material under test.

4.4. Recording and Processing

At the first stage, directivity in the horizontal plane and on-axis frequency responses have been considered for a single MAP. They have been obtained by placing a 1/2" electrostatic microphone at 1 meter and rotating the MAPs with a computer controlled rotating table. Secondly, spatial-time measurements are carried out by sampling a portion of the emitted wave field along a parallel line with respect to the MAPs (see Figure 4). This recording stage has consisted of a 200 microphone array with 1 cm spacing, which is sufficiently below the theoretical Nyquist sampling limit spacing of 9 cm (half the distance between exciters). For implementing such an array, a single 1/2" electrostatic microphone on a computer controlled linear sliding table has been used.

Three stimuli have been employed in the spatial-time measurements. Firstly, the central exciter on the third of the five MAPs is excited to characterize the single-excited MAP operation when changing boundary conditions. Secondly, a synthesized point source is rendered by means of the WFS algorithm. Since additional drive points are excited with respect to the first stimulus, the impact of the boundary condition will be more noticeable. Finally, an axial plane wave by means of WFS algorithm is reproduced by the MAPs. This configuration runs all the exciters with the same amplitude and phase signal, forcing vibration in areas near the boundaries.

In all measurements, Maximum Length Sequences (MLS) were used as excitation signal in order to improve signal-to-noise ratio and minimize unwanted reflections [29]. Once the impulse responses have been recorded, an analysis of the acoustic wave fields is carried out in the spatial-time wavenumber domain, (see [30]) where sampling artifacts, truncation effects and angle-dependent radiation are observed. To that end, the spatial and temporal frequencies are obtained with a double Fourier transformation on the microphone array signals. The obtained

multidimensional signal is plotted in a spatial versus temporal wavenumber graphical representation ($k_x - k$ plot), where k_x and k are the spatial and temporal wavenumbers, respectively. A summary of the theoretical aspects of this analysis is given in the Appendix. For a more detailed description of the tool and its interpretation, refer to [31].

5. Results and Discussion

In this section, measurements following the set-up explained in Section 4.4 are presented and commented upon. They include both elastic boundaries with foam and rubber and also clamped and free boundary conditions which, even though they do not employ such elastic materials, will be addressed as a basis with which to compare elastic boundaries. Firstly, in Section 5.1 on-axis frequency response and directivity is presented, and then, in Section 5.2, a wavenumber domain analysis is performed for three different stimuli.

5.1. On-axis Frequency Response and Directivity

On-axis frequency response and directivity can depict the influence that the boundary conditions may have on the vibration mode radiation of a single MAP. Figure 6 shows the results of eight frequency response measurements combining the experimental conditions and the two elastic materials introduced in section 4. Clamped and free are plotted in Figure 6a as reference responses. Figure 6b depicts the three elastic boundaries responses made with foam, whereas Figure 6c also shows the same elastic boundaries but with rubber material.

As shown in the responses, the main differences are observed at frequencies below 9 kHz, whereas no change is noticed for the rest of the high frequency band. This behaviour is consistent with the radiation of bending wave plates. At low and mid frequencies, the edge radiation is predominant, so a change in its boundary conditions must alter their responses. On the contrary, for high frequencies, all the surface contributes to radiation, where the edge's effect is minimized.

Free and clamped conditions show very different responses up to 700 Hz due to their opposite behaviour on edges (Figure 6a). Regarding the foam material shown in Figure 6b, the three elastic boundaries under test have similar on-axis responses. The flexibility of foam is high enough not to observe moderate differences between elastic boundaries having foam in one or two sides, even if these are not attached to the frame (EB3). Although EB3 response between 2 and 9 kHz is very smooth, there are moderate variations in low frequency. Hence, the most effective foam boundary condition is EF2, where the overall response is the smoothest one. With respect to rubber, Figure 6c illustrates that EB1 response exhibits several peaks and dips, as shown in the clamped condition of Figure 6a. Since rubber is stiffer than foam and EB1 has only one side equipped with damping material, this resemblance makes sense. Although not as severe as EB1, EB2 also presents moderate variations in the on-axis response.

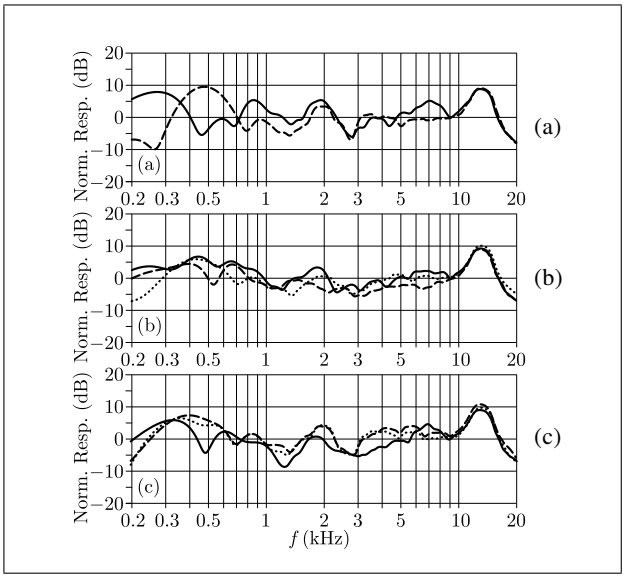

Figure 6. Normalized on-axis frequency response for (a) Free (dashed) and clamped (continuous) conditions, (b) Foam on elastic boundaries: EB1 (continuous), EB2 (dashed), EB3 (dotted), and (c) Rubber on elastic boundaries: EB1 (continuous), EB2 (dashed), EB3 (dotted).

Comparing the three plots of Figure 6, a close resemblance in the low frequency responses of EB3 and free conditions can be observed. This is due to the similar behavior on edges of these two boundary conditions. For mid and high frequencies, both EB2 and EB3 are smoother than free. In general terms, free and clamped conditions give boost to bass power at the expense of smoothness compared to elastic boundaries.

Figure 7 depicts the directivity in the horizontal plane for clamped, free and elastic boundaries as an angle-frequency representation. This plot is useful to observe at a glance the pressure variations as a function of emitting angle for the audio frequency band under consideration.

As expected, since high frequencies are not controlled by panel edges, the directivity response is similar for all boundary conditions, regardless of the elastic material used. This similarity can be perceived in Figure 7 for frequencies above 9 kHz. The pattern that this region exhibits is the one of supersonic modes: forward and backward waves radiate in their direction of propagation producing two lobes pointing in opposite directions. Combined with the weaker main lobe, the overall radiation pattern is a three-lobe broad angle response.

Clamped and free boundary conditions show opposite behaviour for low frequencies. On the one hand, clamped is purely omnidirectional for frequencies up to 400 Hz, whereas free exhibits a broad main lobe. On the other hand, between 1 and 2 kHz, the lobe pattern is different: clamped displays a three-lobe pattern, whereas free has only a centered lobe. In the frequency band of 3–9 kHz and for ±45 degrees, a grid area can be observed, not only for clamped and free but also for the rest of elastic boundaries. Although there is effective sound emission, moderate dips and peaks as direction varies, are occurring. As

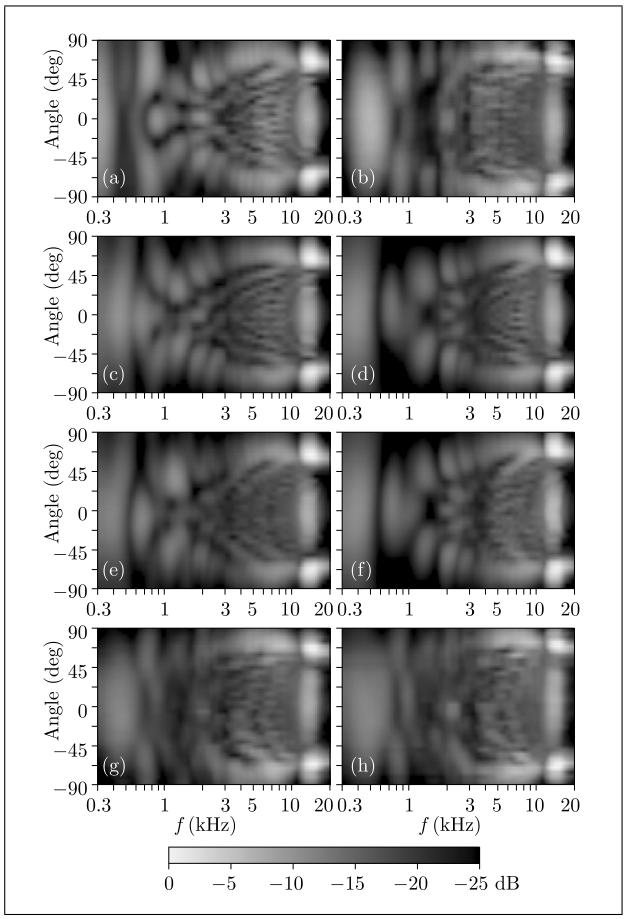

Figure 7. Horizontal plane directivity for (a) clamped and (b) free conditions, EB1 for (c) foam and (d) rubber, EB2 for (e) foam and (f) rubber, EB3 for (g) foam and (h) rubber.

regards elastic materials under test, responses with rubber are more directional than with foam. Figures 7d and f show opposite black areas between 0.5 kHz and 1 kHz, which means that a single main lobe is being emitted. If elastic boundaries are evaluated, it can be seen that EB1 and EB2 have virtually the same directivity responses, in spite of the elastic material employed. As with on-axis response, EB3 is very similar to free condition: energy fall at extreme angles in low frequency is observed as a white spot in both representations.

5.2. Space-Time Wavenumber Domain Analysis

Once the boundary conditions have been tested for their impact on the basic specifications on MAPs, in this subsection, a wavenumber domain analysis of the generated wave field for three different stimuli will be addressed. The three stimuli are designed to progressively increase the vibration of exciters near edges and thus, their influence on the type of edge boundary condition.

5.2.1. Point Source Emanating from the Central Exciter

This configuration drives only one exciter on the third of the five MAPs, so their behaviour will characterize the distributed mode loudspeaker operation when changing the boundary conditions. Also, the created wave field will help in comparing a synthesized version by running the WFS algorithm.

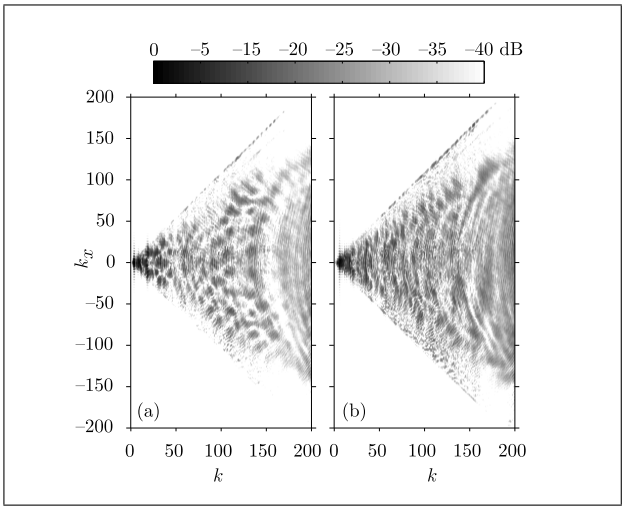

Figure 8. Wave field emitted by the central transducer in the $k_x - k$ representation for (a) clamped and (b) free boundary conditions.

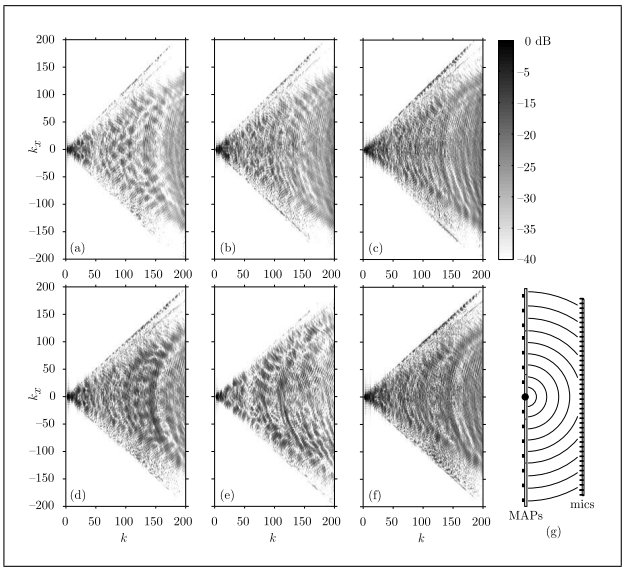

Figure 9. Wave field emitted by a single transducer in the $k_x - k$ representation for elastic boundaries with different elastic materials. Foam on (a) EB1, (b) EB2, (c) EB3. Rubber on (d) EB1, (e) EB2, (f) EB3. (g) Experiment graphical description.

Figure 8 depicts the wave domain representation for clamped and free conditions. Considering that the ideal situation is when several spatial components are emitted for different frequencies, a pure black triangle must be the basis to compare the rest of the responses. According to this, the clamped condition presents a rough distribution of energy within the theoretical triangle. When listening to such a wave field, strong pressure variations would be perceived both in frequency and on moving inside the listening area.

Elastic boundaries show better responses in the $k_x - k$ representations than pure clamped and free (Figure 9). In

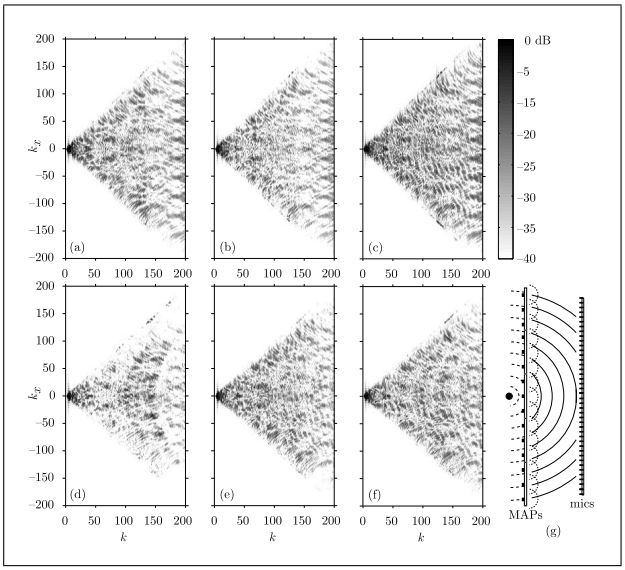

Figure 10. Wave field of a centered synthesized virtual source, centered 0.5 m behind the array, in the $k_x - k$ representation for elastic boundaries with different elastic materials. Foam on (a) EB1, (b) EB2, (c) EB3. Rubber on (d) EB1, (e) EB2, (f) EB3. (g) Experiment graphical description.

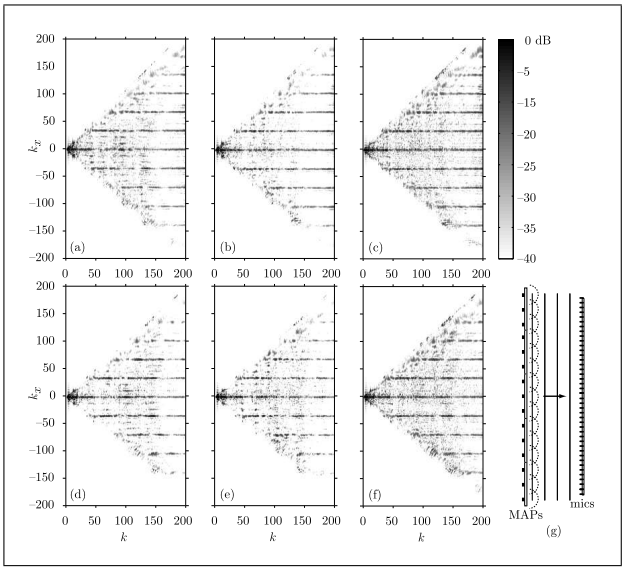

Figure 11. Wave field of an axial plane wave in the $k_x - k$ representation for elastic boundaries with different elastic materials. Foam on (a) EB1, (b) EB2, (c) EB3. Rubber on (d) EB1, (e) EB2, (f) EB3. (g) Experiment graphical description.

order of smoothness, EB3 exhibits a moderate homogeneous response in the spatial-time frequency response for both foam and rubber, Figures 9c and f respectively. The ideal black triangle can be suggested in these responses with more clarity than with other elastic boundaries. As expected, EB2 shows a compromise between the commented EB3 and EB1. Some energy variations start to appear in EB2 and are enhanced for EB1, where only half of the boundaries have elastic materials. Next, the free condition demonstrates a reasonable smoothness but a concentric circular pattern is visible as a superposition. This behaviour is due to the modal nature of the panel, which effect is minimized in elastic boundaries. Finally, as discussed before, clamped shows both an inhomogeneous pattern and a circular pattern, which disturb the generated wave field to an extent.

Foam and rubber materials display noticeable differences for EB1 and EB2, where materials play a role on the emitted wave field. For EB3, since elastic materials serve as foundations in which to support the panel, both responses have close resemblance. Rubber stiffness prevents movement on edges to some extent, as with clamped condition, which causes an inhomogeneous pattern.

5.2.2. Synthesized Point Source by WFS

In this case, from the center to the sides, the amplitude of driving signals will decay progressively. For that reason, the impact of the boundary condition will be more noticeable considering that additional drive points are excited close to edges.

Figure 10 depicts the wave field representation of a virtual point source behind the MAP for elastic boundaries with foam and rubber. Again, rubber responses display moderate variations for EB1 and EB3, whereas EB2 does not show clear deviations with respect to foam. Regarding foam responses, no major differences between EB1 and EB2 are observed, as shown in Figure 10a and b.

5.2.3. Axial Plane Wave by WFS

Such a stimulus will drive all the exciters in MAPs with the same signal (amplitude and phase). Then, the area near the boundaries which is forced to vibrate is at maximum and the potential reflections on the edges will be visible.

Figure 11 shows an axial plane wave field for elastic boundaries with rubber and foam. Plane waves can give additional information to that of the previous sections. In a continuous panel that would contain 15 exciters, edge boundary condition's impact on the panel movement is located before the first exciter and after the last one. In an arrangement of small MAPs that are attached to each other to maintain the transducer spacing, the horizontal extension of each MAP now creates four new areas in the exciter line that will behave according to their boundary conditions. The consequence of such a configuration is the appearance of new undesired replicas of the plane wave field. Therefore, to evaluate the impact of elastic boundaries on such effect, and considering that the distance between the MAPs' center is 0.54 m, two new replicas must be examined at k_x values of $2\pi/0.54 = 11.6\,\mathrm{m}^{-1}$ and $4\pi/0.54$=$23.3\,\mathrm{m}^{-1}$, that are located between the lines that an 18 cm exciter distance creates at spatial frequencies of k_x =0 and $34.9\,\mathrm{m}^{-1}$. The practical consideration of this additional sampling process is that new undesired plane waves will arise on the reproduced wave field. In [31], an exhaustive analysis of this effect is carried out for clamped boundary conditions.

For EB1, both rubber and foam responses have replicas at 11.6 and $23.3\,\mathrm{m}^{-1}$ in Figure 11a and d. Regardless of the elasticity material under test, replicas are visible,

which could be due to the panel area in contact with the frame, acting as clamped. When two elastic materials are used in EB2, unwanted lines are noticeable only for rubber (Figure 11e). The use of two elastic sides and an improved elasticity can minimize the effect of new boundary conditions. Finally, EB3 being the closer to free, has no additional replicas. As a consequence, elastic boundaries can decrease the impact of edge boundary conditions on the reproduced replicas.

6. Conclusion

An empirical study of the impact that the edge boundary conditions have on the radiated wave field has been presented. In addition to the classical clamped and free boundary conditions, elastic boundaries have been addressed as practical boundary conditions that can form a viable technology for a MAP frame. Two elastic materials, representative of soft and hard types within the commercial range, have been employed to develop the elastic boundaries. They were measured in the laboratory to recreate the exact conditions with which they were used in the prototypes.

The major changes have been observed at low and mid frequencies, where the edge radiation was predominant. In general terms, free and clamped conditions boost bass power, at the expense of smoothness compared to elastic boundaries. Wave domain analysis has shown that strong pressure variations would be perceived both in frequency and on moving inside the listening area for these two conditions, which makes them inadvisable in multichannel audio reproduction.

Alternatively, elastic boundaries are a compromise between clamped and free, that can be carried out with different elastic materials. For mid frequencies, on-axis responses were smoother for elastic boundaries than free and clamped, regardless of the elastic material employed. Moderate variations were found in directivity patterns on using clamped and free but not on elastic boundary types 1 and 2, where half or the entire part of the support is filled with foam or rubber. As a consequence, both boundary conditions can be used alternatively with similar results for elastic materials with proper flexibility. Elastic boundary type 3 is a modified version of simply supported, but including elastic material between panel and housing. According to the results, it has no primary advantages over the two other elastic boundaries. Therefore, its use is not recommended, considering the problems that will arise on manufacture in a real MAP frame.

Finally, the appearance of new undesired replicas of the plane wave field when using clamped edges, is minimized for elastic boundaries with flexible materials. As a consequence, with the proper selection of materials for elastic boundaries, the impact of edge boundary conditions on the reproduced replicas can be decreased to a minimum.

Results presented in this paper may help as guidelines in the design and manufacture of new MAPs. They also confirm, with laboratory measurements, the general trend of using elastic materials in panels design.

Appendix

Space-time Wavenumber Domain Analysis

The analysis in the wavenumber domain is an intuitive and physically appealing technique to study wave propagation and diffraction. The transformation of multidimensional wavefields is achieved by means of Fourier transforms in the temporal and spatial domains [31].

The Fourier transform of an unidimensional monochromatic pressure plane wave, propagating in the θ direction at speed c, with respect to time and the spatial coordinate x gives

$$\tilde{P}(k_x, k) = 2\pi P_0(k)\delta(k_x - k_0 \sin\theta), \tag{A1}$$

where the temporal frequency variable ω is expressed in terms of the wave number $k = \omega/c$, k_x is the spatial frequency along the registration axis, and $k_{x_0} = k_0 \sin\theta$ is written as a function of the plane wave travelling direction θ.

The transformed monochromatic plane wave can be plotted in a $k_x - k$ diagram resulting in a delta pulse. The angle β in such representation is related to the angle θ by $\tan\beta = k_x/k = \sin\theta$. In a broad-band plane wave, which includes several frequency components, the $k_x - k$ representation will show a line with angle β since all the wavefronts are travelling at θ angle, and the relation $\tan\beta = k_x/k$ must hold for all delta pulses.

Sampling artifacts

The ideal continuous infinite line of sources and receivers are not possible in practice, which leads to the use of discrete alternatives. First, a continuous distribution of sources is replaced by a set of aligned point sources at discrete positions, a MAP in the context of this paper. This sampling process along the x axis with a Δx interval causes a spatial Nyquist frequency of $k_{x,\max} = \pi/\Delta x$. Assuming plane waves arriving at the x axis at angles up to $\theta = 90^{\circ}$ and a proper time sampling, there is a spatial aliasing which occurs above a certain temporal frequency, named as *spatial aliasing frequency* [5],

$$f_{\mathrm{al}} = \frac{c}{2\Delta x \sin\theta_{\max}}, \tag{A2}$$

where the relation $k_{x,\max}/k_{\mathrm{al}} = \sin\theta_{\max}$ has been used to derive the expression. Note that this equation is only valid if $\theta_{\min} = -\theta_{\max}$ is assumed. The reproduced wave field for a spatially discrete secondary source distribution is a modified version of (A1).

$$\tilde{P}_{\mathrm{al}}(k_x, k) = \sum_{n=-\infty}^{\infty} 2\pi P_0(k)\delta\Big(k_x - k\sin\theta - \frac{2\pi}{\Delta x}n\Big), \tag{A3}$$

which states that the ideal plane wave is repeated in the k_x axis at the n positions $k_x = k\sin\theta + 2\pi n/\Delta x$, each shifted by $2\pi/\Delta x$. The microphone spacing Δx_m is inversely proportional to the spatial resolution capacity of the recording array.

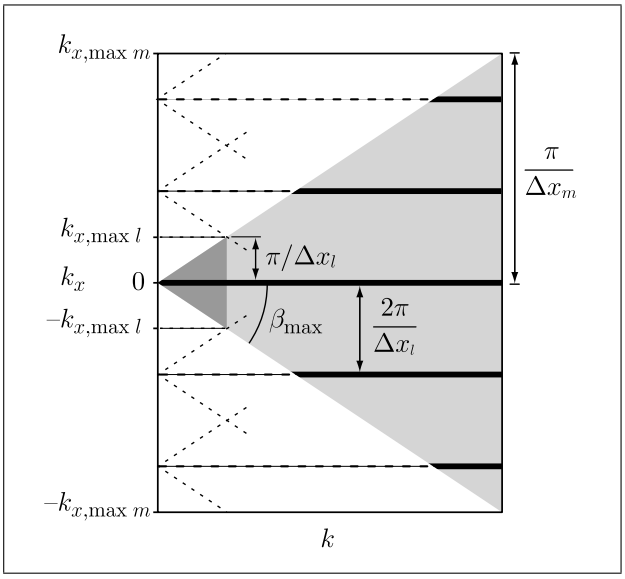

Figure A1. $k_x - k$ representation of a plane wave synthesized by a loudspeaker array and captured by a microphone array, both discrete.

Representation Analysis

For illustration purposes, Figure A1 shows the $k_x - k$ diagram of an axial plane wave ($\theta = \beta = 0$). In such a representation, apart from the main spectrum at $k_x = 0$, there are repetitions at $2\pi/\Delta_x$ positions, according to equation (A3). Let us define $k_{x,\max} = \pi/\Delta x$ as the limit value before entering into the aliased spectrum. For the loudspeaker array, such limit is denoted as $k_{x,\max l}$ and, for the microphone array, as $k_{x,\max m}$.

On the one hand, the loudspeaker array effects can be analyzed in the interval $[-k_{x,\max l}, k_{x,\max l}]$, dark shaded triangle in Figure A1, in which only one spatial period is visible. The wavenumber domain representation of an axial plane wave is zero everywhere except on a single line in k_x=0. On the other hand, the microphone array resolves larger spatial frequencies and determines the highest frequency of the analysis. A limit interval of $[-k_{x,\max m}, k_{x,\max m}]$, light shaded triangle, is shown in Figure A1, which include several spatial periods of the emitting wave. For that reason, a single line on k_x=0 is now repeated for $\pm 2\pi/\Delta x_l$, $\pm 4\pi/\Delta x_l, \ldots$, according to the shifted delta function in equation (A3). In terms of the reproduced wave field, each line represents a series of plane waves arriving at decreasing angles with increasing frequency. When the plane wave contributions are merged, a superposition of plane waves of different angles at different frequencies is created.

Acknowledgements

The authors sincerely thank Prof. Ramón Irles and Prof. José M. Martín for their helpful advice on this manuscript and Dr. María José Muñoz of the Thermomechanical Analysis Laboratory at University of Alicante. This work has been supported by Spanish Ministry of Science and Technology (MCYT) under Project ref. TEC2006-13883-C04-01 and FEDER funds.

References

[1] N. Harris, M. O. Hawksford: The distributed-mode loudspeaker (DML) as a broad-band acoustic radiator. 103rd Conv. Audio Eng. Soc. no. 4526, New York, USA, Sep. 1997.

[2] M. Boone, W. de Brujin: On the applicability of distributed mode loudspeaker panels for Wave Field Synthesis based sound reproduction. 108th Conv. Audio Eng. Soc., Paris, France, Feb. 2000.

[3] E. Corteel: Synthesis of directional sources using wave field synthesis, possibilities, and limitations. EURASIP J. Appl. Signal Process. **2007** (2007) 18.

[4] W. de Brujin, M. Boone: Application of Wave Field Synthesis in life-size videoconferencing. 114th Conv. Audio Eng. Soc. no. 5801, Amsterdam, The Netherlands, Mar. 2003.

[5] A. Berkhout, D. de Vries, P. Vogel: Acoustic control by Wave Field Synthesis. J. Acoust. Soc. Am. **93** (1993) 2764–2778.

[6] E. Start, D. de Vries, A. Berkhout: Wave field synthesis operators for bent line arrays in a 3D space. Acta Acustica united with Acustica **85** (1999) 883–892.

[7] F. Rumsey: Spatial audio. 2nd ed. Focal Press, 2003.

[8] M. Boone: Multi-actuator panels (MAPs) as loudspeaker arrays for Wave Field Synthesis. J. Audio Eng. Soc. **52** (2004) 712–723.

[9] M. Kuster, D. de Vries, D. Beer, S. Brik: Structural and acoustic analysis of multiactuator panels. J. Audio Eng. Soc. **54** (2006) 1065–1076.

[10] B. Pueo, J. Escolano, J. J. López, S. Bleda: Analysis of edge boundary conditions on multiactuator panels. 123th Conv. Audio Eng. Soc., New York, USA, Oct. 2007.

[11] S. Spors, H. Buchner, R. Rabenstein, W. Herbordt: Active listening room compensation for massive multichannel sound reproduction systems using wave-domain adaptive filtering. J. Acoust. Soc. Am. **122** (2007) 354–369.

[12] J. J. López, A. González, L. Fuster: Room compensation in wave field synthesis by means of multichannel inversion. IEEE Workshop on Appl. of Sig. Proc. to. Audio and Acoust. (WASPAA'05), New Paltz, NY, USA, Oct. 2005.

[13] P.-A. Gauthier, A. Berry: Objective evaluation of room effects on wave field synthesis. Acta Acustica united with Acustica **93** (2007) 824–836.

[14] D. de Vries: Sound reinforcement by Wave Field Synthesis: Adaptation of the synthesis operator to the loudspeaker directivity characteristics. J. Audio Eng. Soc. **44** (1996) 1120–1131.

[15] J. Borwick: Loudspeaker and headphone handbook, 3rd ed. Focal Press, 2001.

[16] M. R. Bai, B. Liu: Determination of optimal exciter deployment for panel speakers using the genetic algorithm. J. Sound Vibration **269** (2004) 727–743.

[17] S. Zhang, Y. Shen, X. Shen, J. Zhou: Model optimization of distributed-mode loudspeaker using attached masses. J. Audio Eng. Soc. **54** (295-305) 2006.

[18] E. Y. Prokofieva, K. V. Horoshenkov, N. Harris: The acoustic emission of a distributed mode loudspeaker near a porous layer. J. Acoust. Soc. America **111** (2002) 2665–2670.

[19] E. Corteel, U. Horbach, R. Pellegrini: Multichannel inverse filtering of multiexciter distributed mode loudspeakers for wave field synthesis. 112th Conv. Audio Eng. Soc. no. 5611, Munich, Germany, May 2002.

[20] R. van Zon, E. Corteel, D. de Vries, O. Warusfel: Multiactuator panel (MAP) loudspeakers: how to compensate for their mutual reflections? 116th Conv. Audio Eng. Soc. no. 6052, Berlin, Germany, May 2004.

[21] J. A. Angus: Distributed mode loudspeaker resonance structures. 109th Conv. Audio Eng. Soc. no. 5217, Los Angeles, USA, Sep. 2000.

[22] S. P. Timoshenko, S. Woinowsky-Krieger: Theory of plates and shells, 2nd ed. Mc Graw Hill, 1959.

[23] A. C. Ugural: Stresses in plates and shells, 2nd ed. Mc Graw Hill, 1999.

[24] A. W. Leissa: Vibration of plates. Acoustical Society of America, 1999.

[25] E. Prokofieva, K. V. Horoshenkov, N. Harris: Intensity measurements of the acoustic emission from a DML panel. 112th Conv. Audio Eng. Soc. no. 5609, Munich, Germany, May 2002.

[26] M. R. Bai, T. Huang: Development of panel loudspeaker system: Design, evaluation and enhancement. J. Acoust. Soc. America **109** (2001) 2751–2761.

[27] S. A. Hambric: Structural acoustic tutorial, Part 1: Vibrations in structures. Acoustics Today **2** (2006) 21–33.

[28] M. E. Brown: Introduction to thermal analysis. Techniques and applications, 2nd ed. Springer, 2001.

[29] J. Vanderkooy: Aspects of MLS measuring systems. J. Audio Eng. Soc. **42** (1994) 219–231.

[30] R. Rabenstein, P. Steffen, S. Spors: Representation of two-dimensional wave fields by multidimensional signals. Signal Processing **86** (2006) 1341–1351.

[31] B. Pueo, J. J. López, J. Escolano, S. Bleda: Analysis of multiactuator panels in the space-time wavenumber domain. J. Audio Eng. Soc. **55** (2007) 1092–1106.